Supplementary Materials

Table S1: The predictors for each PC and associated statistical models.

			model
PC1	x_1	Sep SST Southwest Pacific (20.5 °–42.5 °S, 115.5 °–142.5 °W)	$y=0.5x_1+0.52x_2$
	x_2	Oct SST Sargasso Sea (30.5 °–40.5 °N, 45.5 °–60.5 °W)	
PC2	x_1	Oct Snow depth Eastern Siberia (57 °–70 °N, 110 °–170 °E)	$y=0.38x_1+0.38x_2+0.39x_3$
	x_2	Oct Sea ice North to Barents Sea (82 °–90 °N, 45 °–130 °E)	
	x_3	Sep-Oct Soil moisture India Peninsula (15 °–30 °N, 70 °–90 °E)	
PC3	x_1	Oct Soil moisture Indo-China Peninsula (20 °–30 °N, 92.5 °–100 °E)	$y=0.58x_1-0.44x_2$
	x_2	June-Aug SST Gulf of Alaska (35 °–60 °N, 135 °–180 °W)	
PC4	x_1	Oct Sea ice Chukchi Sea (73 °–77 °N, 160 °–180 °W)	$y=-0.55x_1+0.39x_2-0.37x_3$
	x_2	Oct Soil moisture Kamchatka peninsula (60 °–67 °N, 160 °–178 °E)	
	x_3	Aug-Sep SST Arabian Sea (25 °S–20 °N, 50 °–93 °E)	

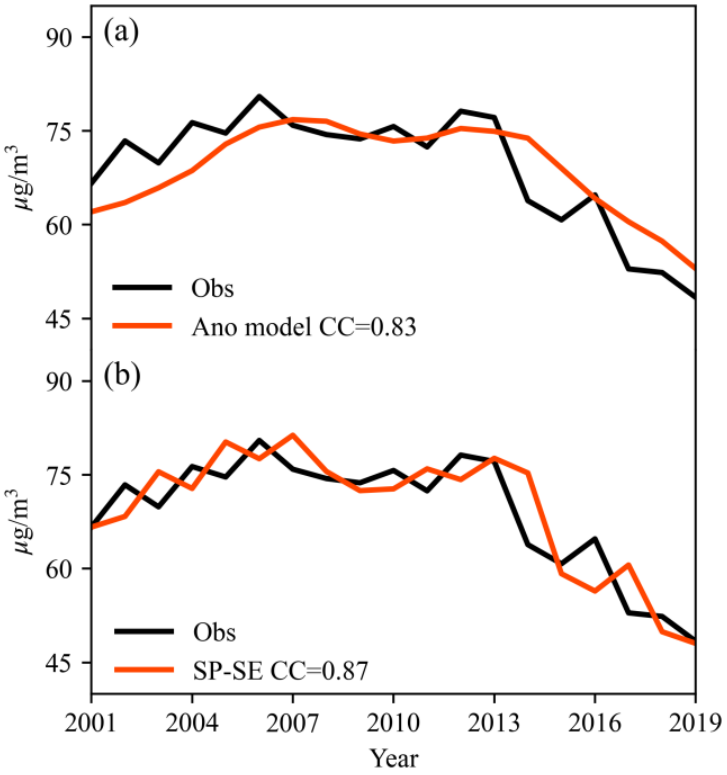

Figure S1: Variation in the reanalysis (black) and predicted winter-mean $PM_{2.5}$ (orange) by anomaly model (a) and SP-SE (b) in east of China from 2001 to 2019.

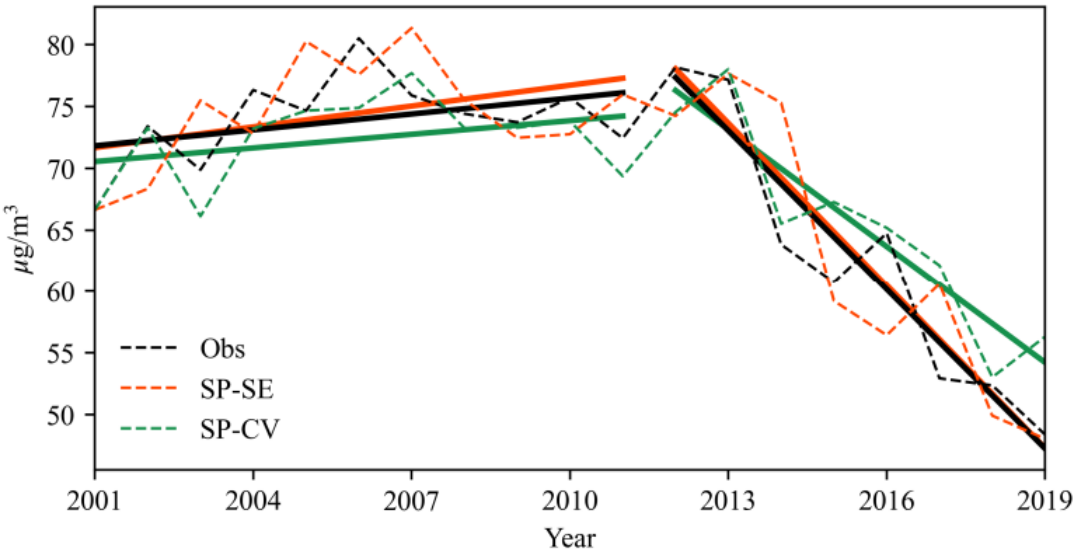

Figure S2: Variation in the reanalysis (black) and predicted winter-mean $PM_{2.5}$ by SP-SE (orange) and SP-CV (green) in east of China from 2001 to 2019. The solid lines indicate the linear trend during 2000-2011 and 2012-2020 respectively.

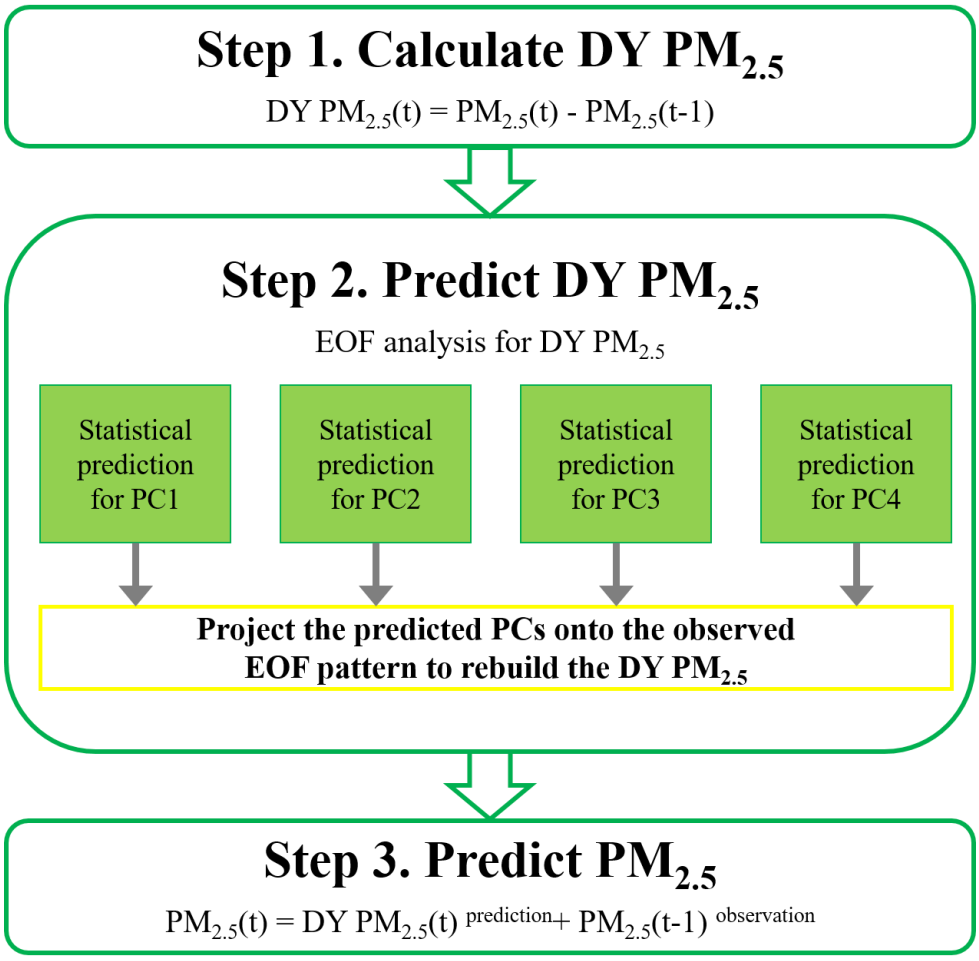

Figure S3: Flowchart of steps to build SP-CV model.

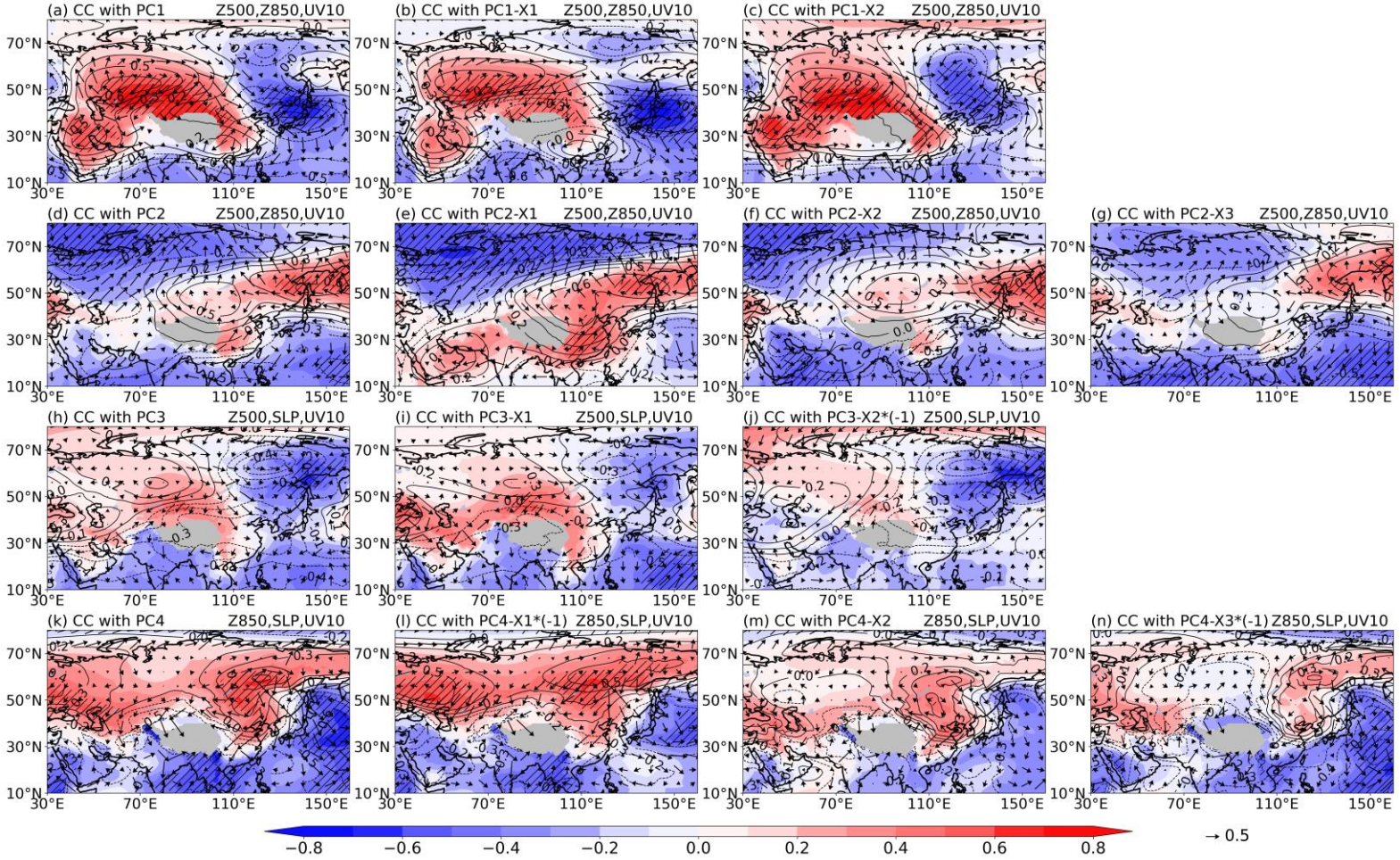

Figure S4: Correlation coefficients between each predictand (a, d, h, k), their predictors: (b-c, e-g, i-j, l-n) and observed DY of atmospheric circulations in winter. The atmospheric variables involved 10m wind (arrows in panel a-n), Z500 (contours in panel a-j) and Z850 (shading in panel a-g and contours in panel k-n) and SLP (shading in panel h-n). The predictor in panel (j, l, n) was multiplied by –1 before calculating the correlation coefficient. The slashes indicate CCs exceeding the 95% confidence level.